

# Demultiplexing of Interferometrically Interrogated Fiber Bragg Grating Sensors Using Hilbert Transform Processing

Kent B. Rochford, *Member, IEEE, Member, OSA*, and Shellee D. Dyer, *Member, IEEE*

**Abstract**—The peak reflectance wavelengths of gratings with reflectance maxima separated by less than 2 nm can be accurately determined through a demultiplexing method based on Hilbert transforms of interferograms. We demonstrate a wavelength demultiplexing of three fiber Bragg gratings (FBG's) with less than 4 pm crosstalk and repeatability and less than 19 pm uncertainty. We anticipate that a large number of gratings can be demultiplexed with a single broadband source and a single receiving interferometer, provided that the interferogram is sampled at accurate intervals slightly above the Nyquist rate.

**Index Terms**—Hilbert transforms, interferometry, optical fiber, sensor, wavelength division multiplexing (WDM), wavelength measurement.

## I. INTRODUCTION

FIBER Bragg grating (FBG) sensors can be easily multiplexed by cascading several sensors with different peak reflectance wavelengths and applying a variety of wavelength demultiplexing methods [1]. For example, the response from all sensors can be simultaneously measured with an optical spectrum analyzer, or individual sensors can be sequentially interrogated by optical bandpass filtering before detection.

Recently, FBG sensor arrays have been demultiplexed by passing the light reflected from the array through a scanning Michelson interferometer and processing the resulting interferogram to determine peak wavelengths. Davis and Kersey [2] reported 15 pm wavelength resolution (for gratings with reflectance near 1500 nm) using an electrical spectrum analyzer to process interferograms formed from 10 cm optical path difference (OPD) scans. Flavin [3] applied Hilbert transform processing to significantly shorten the OPD scan, and reported measuring a single grating's wavelength with 5 pm resolution using a 1.2 mm scan. This technique was extended to the demultiplexing of two gratings separated by 260 nm (gratings fabricated for 1.3 and 1.56  $\mu\text{m}$  reflection wavelengths) [4].

We have determined that the Hilbert transform method is capable of accurately measuring wavelengths that are spaced much more closely. By optimizing sampling rate, reducing sampling jitter, and increasing the interferometer scan length, we demonstrate the demultiplexing of gratings with wavelength differences of 2 nm or less. It is possible to measure these wavelengths with uncertainty approaching 1 pm using

this technique. Also, we discuss processing tradeoffs and show how accuracy is affected by the grating wavelength separation, scan length, and dynamic range. This method appears useful for measuring a very large number of densely multiplexed wavelengths reflected by gratings illuminated by a single broad-band source.

## II. WAVELENGTH DEMULTIPLEXING AND MEASUREMENT

Light reflected from FBG's is passed through a Michelson interferometer (Fig. 1), and the interferogram formed as the mirror is scanned through length  $L$  is periodically sampled to form the series  $S_i$ . Using Hilbert transforms, a time series of real data  $S_i$  can be converted to a discrete analytic sequence  $A_i \exp[j\phi_i]$  ( $i = 1$  to  $i_{\text{max}}$ ) [5]–[7]. In our example, the series  $A_i$  corresponds to the temporal coherence of the reflected light, and  $\phi_i$  are the instantaneous phases of the sinusoidal fringe pattern. Since frequency  $\omega = d\phi/dt$ , the mean frequency is found by calculating the slope of  $\phi_i$  and scaling by the sampling period  $\Delta t = (L_i - L_{i-1})/c$ . The mean wavelength of the light interfering in the Michelson interferometer is then  $\lambda = 2\pi c/\omega$ , where  $c$  is the velocity of light.

The Hilbert transformation from real data  $S_i$  to the analytic sequence  $H_i (= A_i \exp[j\phi_i])$  can be accomplished using fast Fourier transforms (FFT's). To determine the wavelength when only one grating is present, an FFT is performed on the interferogram, the coefficients for all nonpositive frequencies are set to zero, and an inverse FFT taken to yield  $H_i$ . Because the modified spectrum is single-sided, the data set  $H_i$  resulting from the inverse FFT is complex. At each point  $i$ , the instantaneous phase is found using  $\phi_i = \tan^{-1}[\text{Im}(H_i)/\text{Re}(H_i)]$ . The slope of the phase series is found by fitting the  $\phi_i$  to a line, and the mean wavelength is calculated from the slope of  $\phi$ .

If the optical signal is composed of reflections from several wavelengths, the process will provide the mean wavelength of the reflection spectrum. However, if the wavelengths are sufficiently separated, an individual wavelength can be measured by isolating the important frequency components from that wavelength after the initial FFT of the data set  $S_i$  [4]. Only significant Fourier coefficients of the target wavelength are preserved and all other coefficients are set to zero. An inverse FFT is performed on this modified spectrum,  $\phi_i$  is formed, and  $\lambda$  is calculated from the slope of  $\phi$ . To demultiplex signals from several gratings, the spectral windowing and inverse FFT process is then repeated for each grating to form unique sets

Manuscript received November 6, 1998.

The authors are with the Optoelectronics Division, the National Institute of Standards and Technology, Boulder, CO 80303 USA.

Publisher Item Identifier S 0733-8724(99)03960-2.

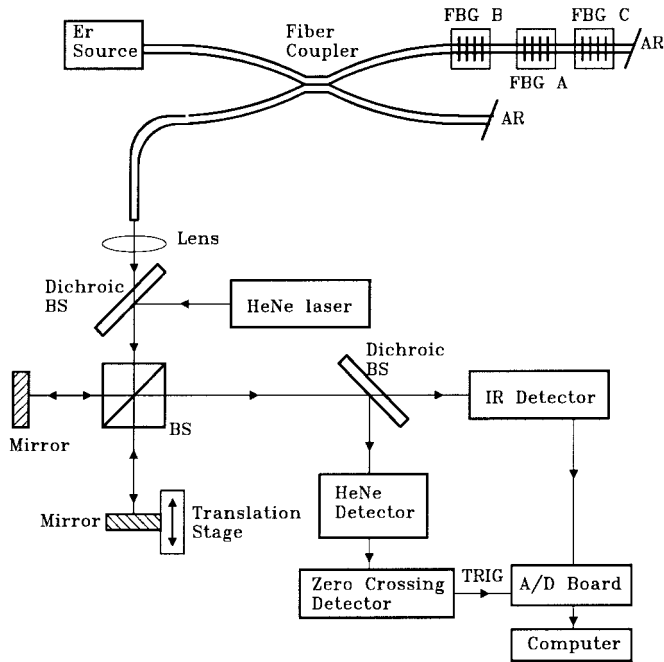


Fig. 1. Experimental apparatus for wavelength division multiplexing and wavelength measurement of FBG sensor signals.

$\phi_i$  that are used to determine each peak reflection wavelength. The process is schematically depicted in Fig. 2.

The number of Fourier components preserved during spectral windowing of the FFT data greatly affects demultiplexing performance. The window size must be large enough to capture the desired spectral information and ensure accurate wavelength determination, but increasing the window width can cause crosstalk if neighboring spectral components from another grating are included. For example, for wavelength  $\lambda$ , an OPD scan of length  $L$  yields an interferogram with  $N = L/\lambda$  periods. When the FFT is performed, the positive-frequency spectral information resides in bins near  $N$ . If two wavelengths separated by  $\Delta\lambda$  are present in an interferogram scan with  $L \gg \lambda$ , each can be accurately measured if  $\Delta\lambda > \lambda^2 b/L$  where  $b$  is the number of FFT bins needed to accurately determine the reflection wavelength of a single grating.

The minimum number of bins required to accurately extract the wavelength is influenced by several factors. FFT's are discrete, so if the wavelength does not exactly correspond to a Fourier component, information is spread among neighboring components, and  $b$  must be chosen to accommodate this spectral leakage. The number  $b$  of bins must be increased when FBG bandwidths are comparable to FFT resolution (bin separations correspond to  $\approx \lambda^2/L$  with Nyquist sampling), suggesting that grating bandwidth should be minimized to maximize grating multiplexing. Sampling jitter and noise also spread spectral information, and increase the window size needed to accurately determine  $\lambda$ .

While jitter, noise, and grating bandwidth contributions to  $b$  approximately scale with  $L$ , the contribution from spectral leakage is not necessarily proportional to  $L$ . Thus, increasing the OPD scan length  $L$  can provide some decrease

in wavelength spacing when spectral leakage is significant. If the scan length is longer than the coherence length of the grating spectrum, however, the resulting phase waveform may exhibit discontinuities where the interferogram has zero visibility. Uncorrected, this can lead to erroneous wavelength estimates, but the discontinuities can be eliminated with additional processing (e.g., phase unwrapping) or the phase slope can be found between discontinuities. While our method does not require symmetric interferograms, approximate centering of the interferometer scans about the zero OPD location maximizes the scan length between discontinuities.

Practical increases in sampling rate, however, do not significantly improve resolution. For a given array size, oversampling provides more high-frequency spectral content in the FFT but contributes little useful information compared to the important spectral features that are windowed and preserved. However, oversampling decreases the spacing of peak spectral components in the FFT if the array size is fixed and this increases the FBG wavelength spacing required for accurate discrimination and measurement. Using the Hilbert process, all the windowed spectral components (both real and imaginary) are used to find the phase, and measurement resolution is not simply limited by the FFT spectral resolution (as is the case in direct Fourier transform spectroscopy). Thus, for our goal of determining peak reflectance wavelengths from a FBG array, sampling just above the Nyquist rate provides the most efficient use of the FFT spectrum and greatest multiplexing density while allowing manageable array sizes.

Since discrete Fourier transforms assume periodic sequences, processing signals with finite extent can lead to biases. To minimize the effect of endpoint discontinuities, we weighted the  $S_i$  data with a Hanning, or  $\cos^2()$ , function to set the endpoints to zero before FFT's are performed. Also, the slope of the phase is found by a linear fit to a truncated set of  $\phi_i$  formed by eliminating the first and last 20% of values.

### III. EXPERIMENT

Fiber Bragg gratings are illuminated with light from a broadband superfluorescent erbium source, and reflected power is directed to a Michelson interferometer by a  $2 \times 2$  coupler (Fig. 1). The detected light is sampled by an externally triggered analog-to-digital (A/D) board, and the sampled voltages stored for processing. A collinear HeNe laser beam also traverses the interferometer, and its detected signal is ac-coupled and sent to a zero-crossing circuit. Each positive-sloped zero-crossing of the HeNe interferogram triggers the A/D board so that as the scanning mirror moves, the interferogram is sampled at OPD increments equal to the HeNe wavelength ( $\lambda = 632.991$  nm in vacuum). The FBG's have nominal wavelengths around 1555 nm; therefore, the interferogram of reflected FBG light is sampled at about 2.5 samples per fringe, just above the Nyquist rate of 2 samples per fringe. An opto-interrupt circuit gates the data acquisition at a fixed mirror position so that the recorded interferogram is approximately centered over the 65 000 point (41 mm OPD) scan.

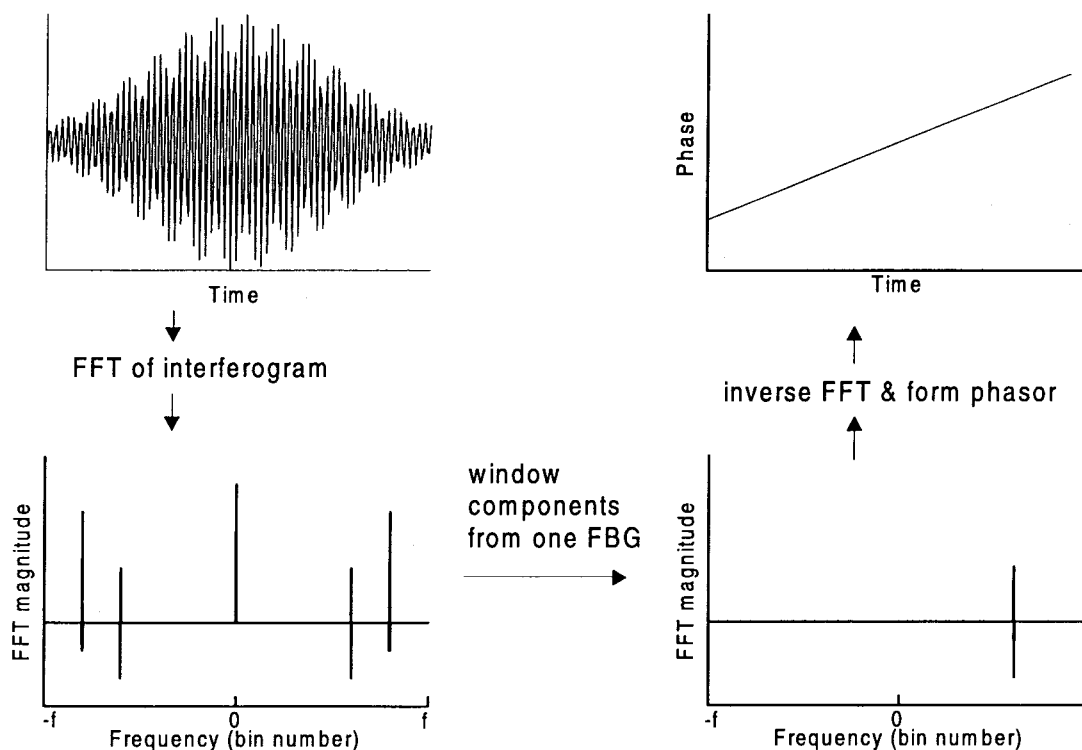


Fig. 2. Processing steps for measuring the wavelength of one FBG from an interferogram of a two wavelength spectrum. After acquiring interferogram data, an FFT is performed. All components at  $f \leq 0$  are set to zero, and only the FFT components from one grating are preserved with windowing. An inverse FFT is performed, the resulting complex data is converted to phasor form, and the phase slope is used to calculate the wavelength. The second grating signal is isolated by repeating the windowing, inverse FFT, and wavelength determination steps.

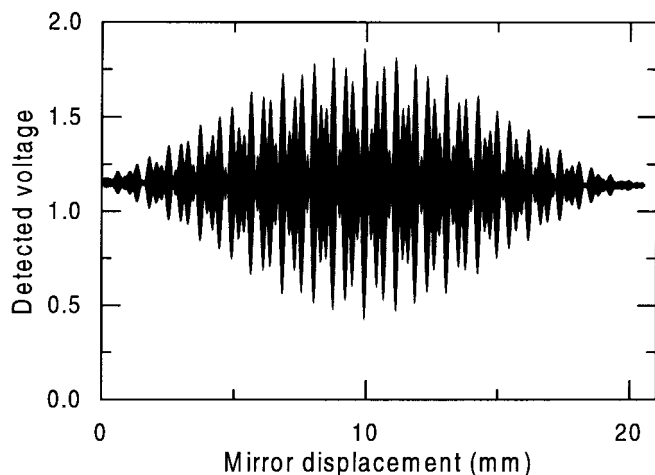


Fig. 3. Sample interferogram from system with three FBG's. All wavelengths are present in the interferogram, and wavelength discrimination is performed by numerically processing this data set.

Up to three FBG's, with nominal peak reflectance wavelengths of 1555, 1558, and 1560 nm, and 0.2 nm bandwidths, were attached to the system in various configurations. An example interferogram of the light reflected from all three gratings is shown in Fig. 3; the beating of the frequencies is clearly evident. The wavelengths calculated using a truncated interferogram of  $2^{15}$  points, corresponding to a 20.7 mm OPD scan, are shown in Table I. These FBG wavelengths were calculated using the vacuum wavelength of the HeNe laser and therefore, neglecting the dispersion of air, represent the

TABLE I  
FBG WAVELENGTHS MEASURED BY HILBERT PROCESSING OF INTERFEROGRAMS

System configuration	FBG's	Measured $\lambda$ (nm)
1	A only	1560.127
2	A & B	1560.130, 1558.165
3	A & B (B attenuated 10 $\times$ )	1560.127, 1558.172
4	A, B, and C	1560.125, 1558.166, 1555.057

vacuum FBG reflection wavelengths. After the FFT of the interferogram, each FBG wavelength was isolated using a  $\sim 2$  nm wide (17 bins) spectral window centered about the peak FFT coefficient (Fig. 4). In one case, the reflected power from grating B was attenuated by a factor of ten through bending loss in the fiber lead. This attenuated reflection example demonstrated that the grating wavelengths can be accurately reconstructed even if the optical source power varied by as much as 10 dB over its output spectrum.

The peak reflectance wavelength of each FBG was also measured using a commercial wavelength meter and comparison with the Table I values yielded differences up to 19 pm. The wavelength meter has 6 pm accuracy when measuring light with a 0.2 nm linewidth, and the slight drift in the wavelength of the multiple-longitudinal mode HeNe laser used for triggering should introduce  $<1$  pm error. Our neglect of the dispersion of air in our wavelength calculations introduces  $<4$  pm error. A major error source lies in coalignment between the HeNe and infrared beams in the interferometer since cosine error in the sampling arises if the beams are not parallel within

TABLE II  
MEASURED WAVELENGTH VERSUS SCAN LENGTH

# data points	OPD scan (mm)	window points	$\lambda_{\text{measured}}$ (nm)	error (pm)
$2^{16}$	41.4	36	1558.172	–
$2^{15}$	20.7	18	1558.173	1
$2^{14}$	10.4	8	1558.168	–4
$2^{13}$	5.2	6	1558.165	–7
$2^{12}$	2.6	4	1559.875	1703

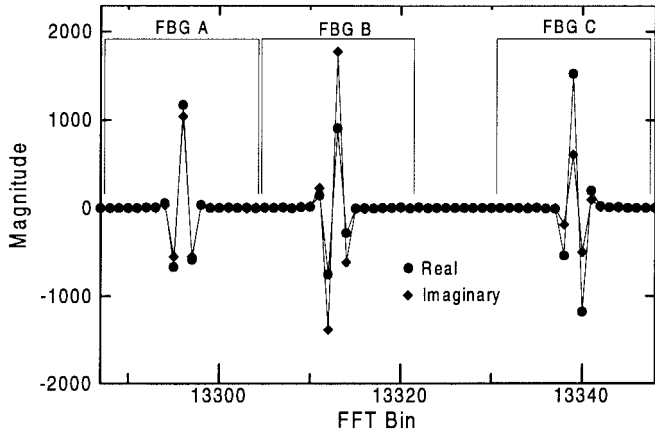


Fig. 4. FFT of a  $2^{15}$  point, three FBG interferogram (Fig. 3). Spectral windows of  $\sim 2$  nm width are shown.

the interferometer. We estimate that the beams are parallel within  $0.3^\circ$  (by resolving beam overlap to within  $100 \mu\text{m}$ ), and this yields  $\leq 22$  pm error in wavelength determination. This bias is repeatable and correctable if the alignment is fixed, or could be eliminated with improved alignment or by using an all-fiber interferometer [2].

Periodic measurements of the same grating configuration over an hour yields 1 pm repeatability. Longer term repeatability of the FBG wavelength measurements is limited by laboratory air temperature fluctuations of  $\pm 1^\circ\text{C}$ . Assuming an FBG temperature coefficient of  $0.01 \text{ nm/K}$ , the temperature changes may cause wavelength variation of up to 20 pm. Comparing measurements taken over one week (for example, the measurements of various grating configurations in Table I) yields better than 7 pm repeatability. However, if the interferometer is realigned between measurements, then the amount of cosine error will change, and influence repeatability.

To illustrate the absence of crosstalk in the reflected signals from multiple gratings, we immersed grating *B* in an ice water bath, while holding the temperature and strain of the other two gratings constant (system configuration 4 from Table I). By adding hot water to the ice bath, we were able to increase the temperature of grating *B* from  $0.0^\circ\text{C}$  to  $73.7 \pm 0.2^\circ\text{C}$ . Over this temperature range, the reflected wavelength of grating *B* changed from  $1557.599$  to  $1558.415$  nm, corresponding to a temperature coefficient of  $0.0112 \text{ nm/K}$ . During this experiment, the measured wavelength of grating *C* remained constant within 3.7 pm, and the measured wavelength of grating *A* changed less than 1.6 pm. At the highest temperature, the reflected wavelengths of gratings *A* and *B* are separated by only 1.4 nm. Despite the proximity

of the two wavelengths, the reflected signals from the two gratings can still be separated by the appropriate windows, and accurate wavelength demultiplexing is still possible.

#### IV. DISCUSSION

Monte Carlo simulations show Hilbert processing does not appear to contribute significant error. Analysis of our interferogram data showed  $< 1\%$  random amplitude noise, and a slowly varying sampling error that ranged over 12% of the sampling period during the scan. For simulations, interferograms were constructed using typical grating parameters and additive Gaussian noise ( $\sigma = 2\%$ ). The simulated interferograms were sampled with Gaussian jitter ( $6\sigma = 12\%$ ), which we determined was more conservative and widely applicable than the slow variation observed in our experiments. Processing of numerous simulated interferograms using the scan lengths and wavelength spacings used in our measurements above gave errors  $\ll 1$  pm. Changes in the interferogram position that move the peak  $\pm 10\%$  from center of the data set, and small changes in window width that do not filter out significant spectral content can change the calculated wavelength by up to 1 pm.

##### A. Scan Length and Window Size

While our demonstration shows that wavelengths separated by 2 nm can be demultiplexed using Hilbert transform processing of  $2^{15}$  points, such spacing is also achievable with shorter scans and smaller data sets. Table II shows the results of extracting the attenuated wavelength of grating *B* in the two-grating interferogram (configuration 3) using smaller data sets selected from the 65 000 point measurement. For comparison, a  $2^{16}$  point data set was also formed by concatenating zeroes to the end of the 65 000 point interferogram. Data were selected so that the interferogram was approximately centered and spectral windows were centered about each FFT peak, but window extent chosen to just overlap at the midpoint between the two FFT peaks; thus window size decreased with the number of points, but the effective window bandwidth is  $\sim 2$  nm for all cases. For the 2.6 mm OPD scan ( $2^{12}$  points) the wavelengths are clearly unresolvable, but OPD's greater than 1 cm ( $2^{14}$  points) yield useful measurements. As comparison, obtaining 4 pm wavelength resolution directly from the FFT spectrum requires  $2^{20}$  points, or a 66 cm OPD scan, using the same sampling rate.

Fig. 5 shows the effect of varying window size and window centering. The  $2^{14}$  points from the single FBG measurement interferogram (configuration 1) were processed with various windows and the resulting wavelength compared to the 12 bin window ( $\sim 2.8$  nm window) case. For  $2^{14}$  points, the

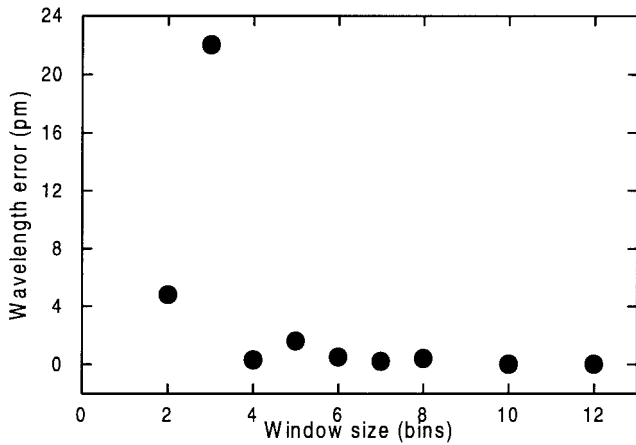


Fig. 5. Error in wavelength determination for various spectral window sizes using  $2^{14}$  point data sets.

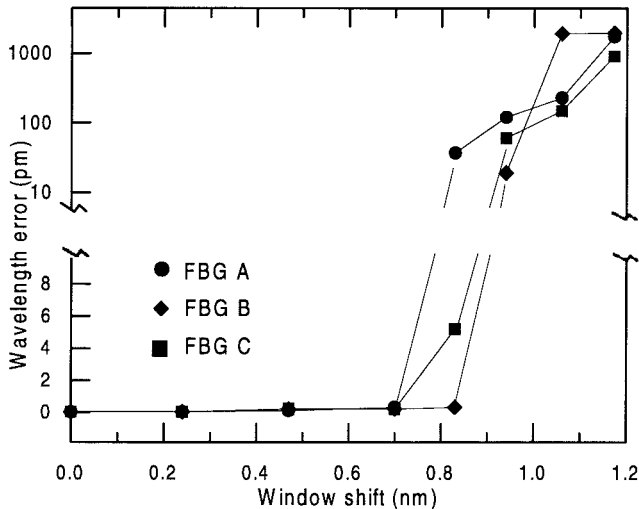


Fig. 6. Error in wavelength determination for fixed bandwidth spectral windows shifted away from the FFT peak.

FBG wavelength yields a nearly half-integer number ( $\sim m + 1/2$ ) of periods in the interferogram and the peak Fourier coefficients are split over two bins. For asymmetric spectra, windows cannot be centered about the spectrum and may cause additional error if necessary spectral components are excluded. For this example, windows of six bins or greater ( $>1.4$  nm) are sufficient, but additional width would be needed to accommodate measurand-induced wavelength shifts. Alternatively, windows can be centered after each measurement by searching the FFT spectrum for peaks and automatically placing windows at appropriate positions.

### B. Dynamic Range

The dynamic range, or the change in wavelength that can be accurately detected, can be estimated by processing data with a shifting window position. Wavelengths from the three grating interferogram (configuration 4) were found using  $2^{15}$  points and  $\sim 2$  nm windows (16 bins). These were compared to calculations made as the window centers were moved to longer wavelengths to approximate the case in which all grating

wavelengths decrease by equivalent amounts. Fig. 6 shows the change in measured wavelength for each case (the FFT spectrum along with the initial (zero-shift) window positions is shown in Fig. 4). Large shifts cause large errors as the windows exclude significant spectral information or include components from neighboring wavelengths. For window centers shifted up to 0.7 nm there is no perceptible change in measured wavelength, but error rapidly increases as window shift increases. Since resolution of less than a few picometers is possible with this method, the dynamic range is in excess of 200, but can be tailored as needed by appropriate grating spacing.

## V. CONCLUSIONS

Closely spaced wavelengths reflected from fiber Bragg gratings can be accurately demultiplexed using Hilbert processing by sampling just above the Nyquist rate and minimizing sampling jitter. Demultiplexing of grating wavelengths separated by 1.4 nm was demonstrated. Comparison of this method to wavelength meter measurements shows that the wavelength determination has  $\leq 19$  pm uncertainty. Much of this uncertainty is a bias that arises from limitations in our ability to perfectly coalign the infrared and sampling HeNe beams in the interferometer; if constant, such cosine error is correctable. Random uncertainties arising from sampling laser drift and processing are  $<2$  pm. Wavelength spacing less than 2 nm is possible, though such decreases may reduce the measurement dynamic range, especially in cases where the measurand causes the grating wavelengths to approach each other. Still, it appears likely that many gratings can be densely multiplexed using a single broadband source and receiving interferometer by simply adding a means for low-jitter sampling and software to implement Hilbert processing.

## ACKNOWLEDGMENT

The authors would like to thank J. Wang of the Statistical Engineering Division, the National Institute of Standards and Technology (NIST), Boulder, CO, for determining the noise statistics of interferogram data.

## REFERENCES

- [1] A. D. Kersey, M. A. Davis, H. J. Patrick, M. LeBlanc, K. P. Koo, C. G. Askins, M. A. Putnam, and E. J. Friebele, "Fiber grating sensors," *J. Lightwave Technol.*, vol. 15, pp. 1442–1461, 1997.
- [2] M. A. Davis and A. D. Kersey, "Application of a fiber Fourier transform spectrometer to the detection of wavelength-encoded signals from Bragg grating sensors," *J. Lightwave Technol.*, vol. 13, pp. 1289–1295, 1995.
- [3] D. A. Flavin, R. McBride, and J. D. C. Jones, "Short optical path scan interferometric interrogation of fiber Bragg grating embedded in a composite," *Electron. Lett.*, vol. 33, pp. 319–320, 1997.
- [4] D. A. Flavin, R. McBride, and J. D. C. Jones, "Absolute measurement of wavelengths from a multiplexed in-fiber Bragg grating array by short-scan interferometry," in *Proc. 12th Int. Conf. Optic. Fiber Sensors*, vol. 16, OSA Tech. Dig. Series (Optical Society of America, Washington, DC, 1997), pp. 24–27. See also, "Short-scan interferometric interrogation and multiplexing of fiber Bragg grating sensors," *Opt. Lett.*, to be published.
- [5] R. N. Bracewell, *The Fourier Transform and Its Applications*. New York: McGraw-Hill, 1986, pp. 267–271.
- [6] S. L. Hahn, *Hilbert Transforms in Signal Processing*. Boston, MA: Artech House, 1996, pp. 37–47, pp. 156–159.
- [7] K. B. Rochford and C. M. Wang, "Accurate interferometric retardance measurements," *Appl. Opt.*, vol. 36, pp. 6473–6479, 1997.

**Kent B. Rochford** (S'89–M'91) received the B.S. degree in electrical engineering at Arizona State University, Tempe, in 1982 and the M.S. and Ph.D. degrees in optical sciences at the University of Arizona, Tucson, in 1988 and 1990, respectively.

From 1983 to 1985, he was with 3M Central Research, Maplewood, MN, performing research on electrooptic materials. In 1985, he began graduate research in linear and nonlinear guided-wave optics at the Optical Sciences Center, Tucson. In 1992, he joined the National Institute of Standards and Technology Optoelectronics Division, Boulder, CO, and currently leads the Optical Fiber Sensors project. He is presently engaged in research and development of optical fiber sensors and polarization metrology.

Dr. Rochford is a member of the Optical Society of America (OSA).

**Shellee D. Dyer** (S'88–M'97) received the Ph.D. degree in electrical engineering from the University of Utah, Salt Lake City, in 1996.

She then joined the National Institute of Standards and Technology, Boulder, CO, as a National Research Council Fellow and is currently a member of the Optoelectronics Division. Her current research interests include fiber-optic sensors, low-coherence interferometry, and fiber Bragg grating measurements and characterization.